Supplementary Information

Facile synthesis of N-doped graphene quantum dots as fluorescent sensor for Cr(VI) and folic acid detection

Chu-Sen Ni,‡[a] Wen-Jie Zhang,‡[a] Wen-Zhu Bi,*[a,b] Ming-Xia Wu,*[a,b] Su-Xiang Feng,*[b,c,d] Xiao-Lan Chen[e] and Ling-Bo Qu[e]

[a] School of Pharmacy, Henan University of Chinese Medicine, Zhengzhou, 450046, China. E-mail: mxwu711@163.com.

[b] Henan Engineering Research Center of Modern Chinese Medicine Research, Development and Application, Zhengzhou, 450046, China.

[c] Academy of Chinese Medical Sciences, Henan University of Chinese Medicine, Zhengzhou, 450046, China. E-mail: fengsx221@163.com.

[d] Collaborative Innovation Center for Chinese Medicine and Respiratory Diseases co-constructed by Henan province & Education Ministry of P. R. China, Zhengzhou, 450046, China.

[e] College of Chemistry, Zhengzhou University, Zhengzhou, 450001, China.

‡ These authors contributed equally to this work and should be considered as co-first authors.

Corresponding E-mail: biwenzhu2018@hactcm.edu.cn

Table of Contents

1. Table S1 Comparison of carbon dots-based fluorescence probes for Cr(VI) detection

No.	Carbon Dots	Linear range	Limit of detection	Fluorescence quantum yield	Response time	Reference
1	EDTA/DMF derived CDs	0-0.1 M	10 μM	/	5 min	*Front. Chem.*, 2020, **8**, 595628
2	MR-CDs	0.2-50 μM	20 nM	18%	10 min	*Nanomaterials*, 2020, **10**, 1924
3	B,N-CDs	0.3-500 μM	0.24 μM	59.01%	8 min	*Spectrochim. Acta. A Mol. Biomol. Spectrosc.*, 2020, **243**, 118807
4	BNCDs	0-100 μM	0.41 μM	/	/	*Carbon*, 2021, **182**, 42
5	N,P-CDs	0.05-3 μM	26 nM	1.8%	10 min	*Microchem. J. ,* 2021, **166**, 106219
6	CDs	120 nM-200 μM	37 nM	/	10 min	*Microchem. J.*, 2021, **169**, 106552
7	BH@CD	0-20 μM	66 nM		/	*Sens. Actuators B Chem.*, 2021, **348**, 130662
8	N,S-CDs	0-120 μM	1.04 μM	4.37%	5 min	*RSC Adv.* 2021, **11**, 35946
9	af-CDs	0.8-80.0 μM	242 nM	2.3%	1 min	*J. Photochem. Photobiol. A Chem.*, 2021, **417**, 113359
10	NH_2- $mSiO_2$@CDs	0.5-9 μM	5 nM	/	1 min	*J. Hazard. Mater.*, 2021, **415**, 125699
11	S,N-CDs	0.03-50 μM	21.14 nM	17%	3 min	*Microchem. J.*, 2021, **167**, 106284
12	Cs-CDs	1-130 μM	0.91 μM	58%	/	*Nano*, 2021, **16**, 2150103
13	CA/WS-CDs	10-50 mg/L	7.6 mg/L	/	/	*Environ. Sci.: Nano*, 2021, **8**, 3331
14	PGP-CDs	0.1-100 μM	4 nM	15%	1 min	*J. Mol. Liq.*, 2022, **346**, 117088
15	O-phenylenediamine/ DL-Thioctic acid derived CDs	0-60 μM	0.64 μM	21.82%	./	*Colloids Surf. A Physicochem. Eng. Aspects* , 2022, **638**, 128164
16	Single-layered GQDs	3-75 μM	0.1 μM	23.8%	/	*Chem. Eng. J.*, 2022, **435**, 131833
17	CNF-TCDs3	0-15 mg/L	0.15 mg/L	/	/	*Chem. Eng. J.* , 2022, **432**, 134202

18	CF-CDs	5-50 μM	1.7 ppm	/	/	*J. Basic Microbiol.*, 2022, **62**, 455
19	Poria cocos polysaccharide/ethylene diamine derived CDs	1-100 μM	0.25 μM	4.82%	25 min	*J. Pharm. Anal.*, 2022, **12**, 104
20	R-CDs	0.3-50 μM/0.03-3 μM	80 nM/9.1 nM	22.96%	10 min	*Biosensors*, 2022, **12**, 432
21	N-CDs	1-80 μM	00.61 μM	31%	/	*Nano*., 2022, **17**, 2250086
22	N,S-CDs	0-0.588 ppm	0.038 ppm	/	5 min	*Chem. Pap.*, 2022, **76**, 7793
23	L-tartaric acid/citric acid/urea derived CDs	0.8-189 μM	0.16 μM	20.5%	instantaneous	*Spectrochim. Acta. A Mol. Biomol. Spectrosc.*, 2022, **278**, 121343
24	N,P-CDs	0.68-87.38 μM	0.18 μM	11.3%	10 min	*J. Anal. Test.*, 2022, **6**, 335
25	CD-600	0.1-0.4 nM	0.04 nM	2-3%	/	*Chem. Eng. J.*, 2022, **446**, 137171
26	SNCDs	5 nM-25 μM	5 nM	17.67%	/	*J. Lumin.*, 2022, **244**, 118767
27	N,S-doped CDs	3.8-38.9 μM	47.2 nM	16%	/	*Anal. Bioanal. Chem.*, 2022, **414**, 7253
28	N-CQDs	0-15 μM	300 nM	18%	4 min	*Diam. Relat. Mater.*, 2022, **126**, 109138
29	banana stem/phosphoric acid derived CDs	10-30 μM	2.4 μM	15.11%	20 sec	*Mater. Chem. Phys.,* 2022, **286**, 126133
30	N-CQDs	0 -100 μM	2.1 μM	22.1%	/	*Anal. Chim. Acta*, 2022, **1195**, 339478
31	CE-CDs	0-500 μM/0-5 μM	1.56 μM/23 nM	72%	3 min	*Ecotox. Environ. Saf.*, 2022, **244**, 114069
32	FW-CDs	0.1-60 μM	0.07 μM	14.8%	30 min	*Molecules*, 2022, **27**, 1258
33	Citric acid/glutamic acid derived CDSs	0.5-400 μM	0.1 μM	48.41%	1 min	*J. Fluoresc.*, 2022, **32**, 2343
34	Arg-L-CQDs	0-400 μM	0.8625 μM	/	/	*Macromol. Chem. Phys.*, 2023, **224**, 2200380
35	N,Cl-doped CQDs	5-350 μM/250-600 μM/300-850 μM	0.28 μM/0.87 μM/0.90 μM	3.58%	5 min	*Colloids Surf. A Physicochem. Eng. Aspects*, 2023, **669**, 131471
36	N/S-GQDs	1-100μM/0.5-10 μM	0.01 μM/0.4 μM	22%	10 min	*Langmuir*, 2023, **39**, 1538

37	N-CQDs	0-40 μM	0.16 μM	/	/	*J. Fluoresc.*, 2023, **139**, 1573
38	BCD1	0-220 μM	0.242 μM	8.9%	15 min	*ACS Omega*, 2023, **8**, 6550
39	CQDs	20-200 μM	1.4 μM	5.6%	/	*Packag. Technol. Sci.,* 2023, **36**, 465
40	N,Zn-doped CDs	0.005-0.135 μM	0.47 nM	13.6%	/	*Sensors*, 2023, **23**, 1632
41	N-CDs-CTAC	0.5-1000 μM	40 nM	44.6%	10 min	*Analyst*, 2023, **148**, 2818
42	ILCDs	1-750 μM	0.5 μM	16.34%	35 min	*Ind. Eng. Chem. Res.*, 2023, **62**, 10849
43	S-CDs	10-80 nM	20 nM	3%	/	*J. Environ. Chem. Eng.*, 2023, **11**, 109438
44	**N-GQDs**	**0-50 μM**	**0.80 μM**	**10.9%**	**< 10 sec**	**This work**

2. Table S2 Comparison of carbon dots-based fluorescence probes for FA detection

No.	Carbon Dots	Linear range	Limit of detection	Fluorescence quantum yield	Response time	Reference
1	N,S-GQD-$NaHSO_3$-NaClO	0.5-70 μM	78 nM	77.2%	/	*Food Anal. Methods*, 2019, **12**, 869
2	Amino QDs-Carboxyl GQDs	0.11-22.66 nM	0.09 nM	/	/	*Anal. Bioanal. Chem.*, 2019, **411**, 7481
3	CA/EIP CQDs	1.14-47.57 μM	0.38 μM	/	/	*Spectrochim. Acta. A Mol. Biomol. Spectrosc.*, 2020, **229**, 117931
4	N,S,I-CDs	0.1-175 μM	84 nM	32.4%	5 min	*Spectrochim. Acta. A Mol. Biomol. Spectrosc.*, 2020, **224**, 117444
5	CDs-MCM	0-50 μM	118.73 nM	10.39%	/	*Nano*, 2020, **15**, 2050090
6	HCA-CDs	4-100 μM	0.49 μM	/	5 min	*Microchem. J.*, 2020, **159**, 105364
7	paper@CDs	1-300 μM	0.28 μM	/	12 min	*Anal. Bioanal. Chem.*, 2020, **412**, 2805
8	NGQDs	0.8-80 μM	81.7 nM	/	10 min	*ACS Appl. Mater. Interfaces*, 2021, **13**, 34572

9	C60 FNPs	0-80 µM	0.24 µM	26%	1 min	*Nanotechnology*, 2021, **32**, 195501
10	Carbon Nanodots-Quantum Dots Composite	0.113-906 µM	0.039 µM	/	/	*Food Anal. Methods*, 2021, **14**, 1637
11	N-CDs	0-200 µM	28 nM	26.5%	3 min	*Spectrochim. Acta. A Mol. Biomol. Spectrosc.*, 2022, **268**, 120661
12	PEI-OH-CDs	0.1-100 µM	0.07 µM	25%	5 min	*J. Chin. Chem. Soc.*, 2022, **69**, 486
13	S,O-CNQDs	5-83.3 µM	90 nM	/	5 min	*Arab. J. Chem.*, 2023, **16**, 104520
14	N-CDs	0.1-165 µM	0.04 µM	7.65%	1 min	*Spectrochim. Acta. A Mol. Biomol. Spectrosc.*, 2023, **285**, 121891
15	Gd,N-CDs	0-30 µM	3.43 nM	2.52%	1 min	*Dyes Pigments*, 2023, **209**, 110877
16	Mn,N-CQDs	2-100 µM	0.19 ppm	37%	60 min	*J. Nanopart. Res.*, 2023, **25**, 92
17	N,S,P-CDs	4.85-82.45 µM	0.148 µM	41%	/	*Dalton Trans.*, 2023, **52**, 6551
18	Anhydrous citric acid/ ethylenediamine derived CDs	0-50 nM	6 nM	30%	/	*Microchem. J*, 2023, **188**, 108470
19	**N-GQDs**	**0-200 µM**	**2.1 µM**	**10.9%**	**< 10 sec**	**This work**

3. Materials and instruments

All reagents used in this work showed below were purchased from commercial suppliers without further purification. Soluble starch ($C_{12}H_{22}O_{11}$, CAS: 9005-84-9), L-arginine (L-Arg, $C_6H_{14}N_4O_2$, CAS: 74-79-3), glucose ($C_6H_{12}O_6$, CAS: 50-99-7), starch (($C_6H_{10}O_5$)n, CAS: 9005-25-8), glutathione (GSH, $C_{10}H_{17}N_3O_6S$), serine (Ser, $C_3H_7NO_3$), glycine (Gly, $C_2H_5NO_2$), alanine (Ala, $C_3H_7NO_2$), L-threonine (L-Thr, $C_4H_9NO_3$), L-cysteine (L-Cys, $C_3H_7NO_2S$), L-lysine (L-Lys, $C_6H_{14}N_2O_2$), L-glutamic acid (L-Glu, $C_5H_9NO_4$), L-histidine (L-His, $C_6H_9N_3O_2$), folic acid (FA, $C_{19}H_{19}N_7O_6$), ascorbic acid (AA, $C_6H_8O_6$), vitamin B6 (VB6, $C_8H_{11}NO_3$•HCl), nicotinamide ($C_6H_6N_2O$), citric acid (CA, $C_6H_8O_7$), urea (CH_4N_2O), silver nitrate ($AgNO_3$), aluminum chloride ($AlCl_3$) barium chloride dihydrate ($BaCl_2$•$2H_2O$), calcium chloride ($CaCl_2$), cadmium sulfate 8/3-hydrate ($3CdSO_4$•$8H_2O$), cobalt sulfate heptahydrate ($CoSO_4$•$7H_2O$), chromium (III) trichloride hexahydrate ($CrCl_3$•$6H_2O$), dichromate potassium dichromate ($K_2Cr_2O_7$), cupric sulfate ($CuSO_4$), ferric chloride hexahydrate ($FeCl_3$•$6H_2O$), mercury(II) thiocyanate ($Hg(SCN)_2$), potassium bromide (KBr), potassium chloride (KCl), potassium carbonate (K_2CO_3), potassium iodide (KI), potassium phosphate (K_3PO_4), manganese (II) chloride tetrahydrate ($MnCl_2$•$4H_2O$), sodium perchlorate,($NaClO_4$), sodium fluoride (NaF), sodium sulfate (Na_2SO_4), ammonium chloride (NH_4Cl), nickel(II) chloride ($NiCl_2$), lead(II) nitrate ($Pb(NO_3)_2$), stannous chloride dihydrate ($SnCl_2$•$2H_2O$), zinc sulfate heptahydrate ($ZnSO_4$•$7H_2O$). Sucrose ($C_{12}H_{22}O_{11}$) was obtained from the local supermarket.

Fluorescence spectra were measured by Hitachi F7000 with the slit width of 5/5 nm. Other instruments employed in this work are UV-Visible spectrophotometer (Thermo Evolution 260 Bio), pH Meter (FiveEasy Plus FE28), Transmission electron microscope (TF20), Atomic force microscopy (Bruker Dimension Icon), X-ray powder diffractometer (Bruker D8 Advance), X-ray photoelectron spectrometer (Thermo ESCALAB 250), Fourier transform infrared spectrometer (Perkin Elmer Frontier), Steady-state/transient fluorescence spectrometer, Zeta potential analyzer.

4. Optimization of the hydrothermal reaction conditions for the synthesis of N-GQDs

Carbon sources (glucose, sucrose, soluble starch and starch) (0.15 g) and L-arginine (L-arg, 0.3-1.2 g) were firstly mixed in pure water (12.5 mL) and stirred at 60 °C for 15 min. Then, the mixture was sealed into a 25 mL stainless autoclave lined with Teflon and heated at 180-200 °C for 3-5 h. After that, the mixture was naturally cooled to room temperature and the N-GQDs were obtained by centrifugation at 15,000 rpm for 15 min. The obtained N-GQDs were stored as stock solution at room temperature for further use.

Table S3 Optimization of the hydrothermal reaction conditions.

Entry	Carbon source	Nitrogen source	Temperature (°C)	Time (h)	λ_{max}^{em} (nm)	Fluorescence intensity (a.u.)
1	glucose, 0.15 g	L-arg, 0.9 g	190	4	442	935
2	sucrose, 0.15 g	L-arg, 0.9 g	190	4	439	637
3	soluble starch, 0.15 g	L-arg, 0.9 g	190	4	445	1380
4	starch, 0.15 g	L-arg, 0.9 g	190	4	423	1181
5	soluble starch, 0.15 g	L-arg, 0.3 g	190	4	446	432
6	soluble starch, 0.15 g	L-arg, 0.6 g	190	4	443	816
7	soluble starch, 0.15 g	L-arg, 1.2 g	190	4	439	1245
8	soluble starch, 0.15 g	L-arg, 0.9 g	180	4	425	1043
9	soluble starch, 0.15 g	L-arg, 0.9 g	200	4	444	819
10	soluble starch, 0.15 g	L-arg, 0.9 g	190	3	436	935
11	soluble starch, 0.15 g	L-arg, 0.9 g	190	5	440	1006

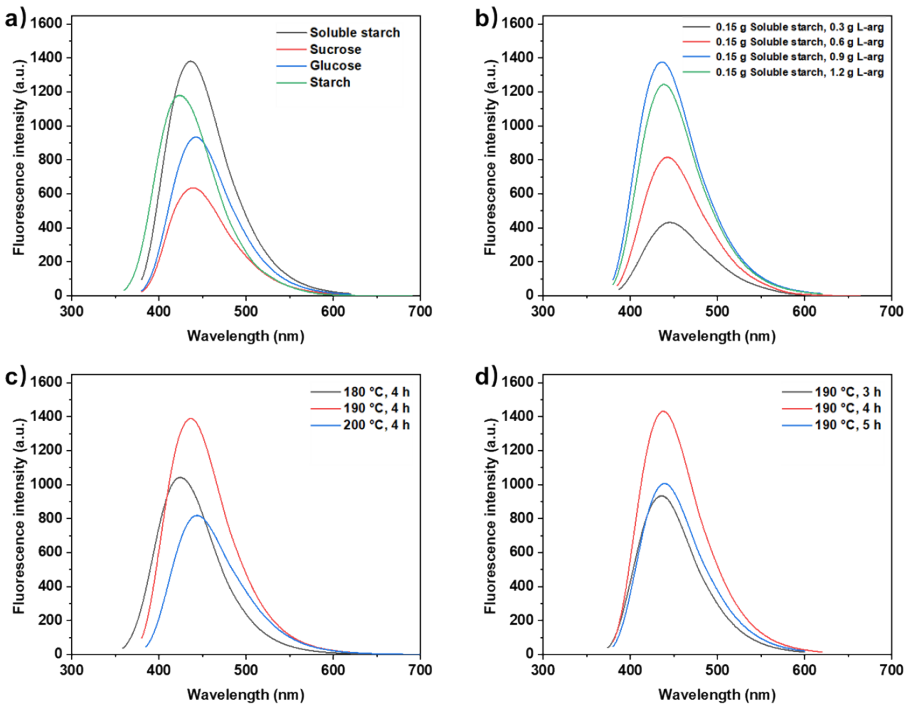

Fig. S1 Fluorescence spectra of the as-synthesized N-GQDs under different conditions in Table S3: (a) entry 1-4; (b) entry 3, 5-7; (c) entry 3, 8-9; (d) entry 3, 10-11.

5. FTIR spectrum of N-GQDs

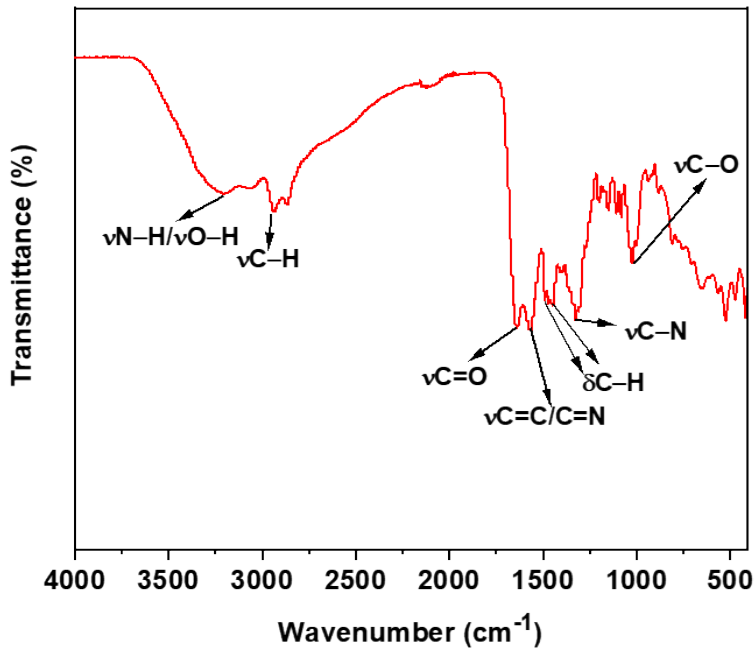

Fig. S2 FTIR spectrum of N-GQDs.

6. Calculation of fluorescence quantum yield of N-GQDs

The fluorescence quantum yield (QY) of N-GQDs was determined by a common method according to previous reports using quinine sulfate in pure water as a reference (QY = 55%). The fluorescence QY value of N-GQDs was calculated as follows:

$$QYt = QYr \times (It/Ir) \times (Ar/At) \times (\eta t/\eta r)^2$$

The subscript "t" and "r" refer to the N-GQDs and quinine sulfate. A is the optical density, I is the integrated emission intensity, and ŋ is the refractive index of the solvent. To get more reliable results, the absorption of the two solutions were adjusted to less than 0.1 to prevent the reabsorption effect.

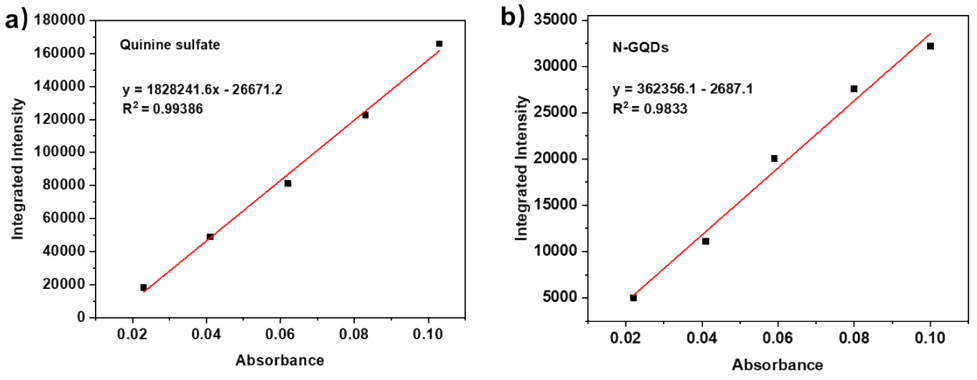

c)

	Quinine sulfate					N-GQDs				
Absorbance	0.022	0.038	0.061	0.082	0.102	0.022	0.041	0.059	0.080	0.100
Integrated Intensity	18296.11	48906.1	81227.1	122660	165966.2	5032.859	11132.78	20046.67	27565.03	32218.84
Excitation (nm)	380					380				
Slope	1828241.6					362356.1				
QY (%)	55					10.9				

Fig. S3 Plots of integrated intensity of Quinine sulfate and N-GQDs.

7. Thermostability, photostability and reproducibility of N-GQDs

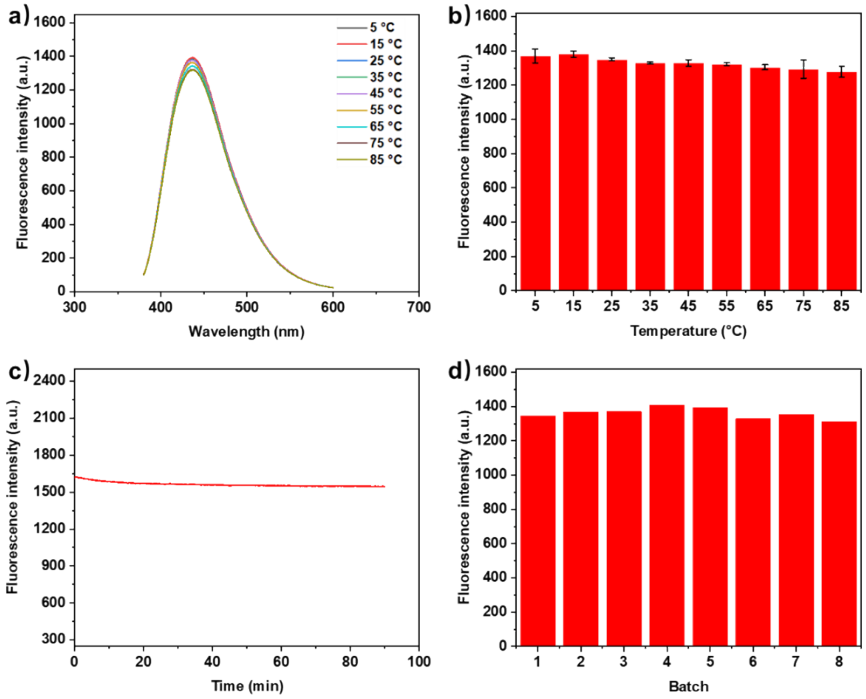

Fig. S4 (a) Fluorescence spectra of N-GQDs under different incubation temperatures; (b-d) fluorescence intensities of N-GQDs at 445 nm: (b) under different incubation temperatures (n = 3); (c) at continuous excitation wavelength of 370 nm; (d) between 8 different batches of N-GQDs.

8. General experimental procedure

Detection of Cr(VI)

N-GQDs stock solution (500 μL) was firstly diluted by pure water (3.0 mL) and different amount of Cr(VI) were added. Then the solutions were further diluted by pure water to 5.0 mL. The concentrations of Cr(VI) in the solutions were 0-175 μM. Then the fluorescence intensities of the mixed solutions were measured and repeated for 3 times. Other cations (Ag^{+}, Al^{3+}, Ba^{2+}, Ca^{2+}, Cd^{2+}, Co^{2+}, Cr^{3+}, Cu^{2+}, Fe^{3+}, Hg^{2+}, K^{+}, Mn^{2+}, Na^{+}, NH_4^{+}, Ni^{2+}, Pb^{2+}, Sn^{2+} and Zn^{2+} (10 mM, 87.5 μL)) and common anions (Br^{-}, Cl^{-}, ClO_4^{-}, CO_3^{2-}, F^{-}, I^{-}, NO_3^{-}, PO_4^{3-}, SCN^{-} and SO_4^{2-} (10 mM, 87.5 μL)) were added under the same conditions.

Detection of FA

N-GQDs stock solution (500 μL) was firstly diluted by pure water (3.0 mL) and different amount of FA were added. Then the solutions were further diluted to 5.0 mL. The concentrations of FA in the solutions were 0-200 μM. Then the fluorescence intensities of the mixed solutions were measured and repeated for 3 times. Other interfering compounds (GSH, Glucose, Ser, Gly, Ala, L-Arg, L-Thr, L-Cys, L-Lys, L-Glu, L-His, AA, VB6, niacinamide, CA and Urea (10 mM, 50 μL)) were added under the same conditions.

Detection of Cr(VI) in actual water samples:

The actual samples selected for the determination of Cr(VI) were tap water, C′eastbon bottled drinking water and lake water. Tap water was collected from laboratory water piping, C′estbon bottled drinking water was purchased from the local supermarket and the lake water was collected from Tianyi Lake in Henan University of Chinese Medicine. The practical water samples were centrifuged at 8000 rpm for 20 min and filtered through a 0.22 μm microporous membrane. Then, different amount of Cr(VI) were added into the above water samples to

calculate the recovery rate and relative standard deviation (RSD). All measurements were repeated for 3 times.

Detection of FA in FA tablet:

FA tablets (5 mg/tablet) were purchased at a local drugstore. The average weight of 10 tablets was calculated after thorough pulverization into fine powder. An amount of FA powder equal to the mass of one FA tablet was accurately weighed and dissolved in 20 mL pure water with ultrasonic assistance. The solution was centrifuged for 20 min at 8000 rpm and filtered through 0.22 μm membrane syringe filters. The working solution was prepared by diluting the sample solution with pure water to maintain the concentration of the working solution within the linear range. Then, different amount of FA were added into the above working solution to calculate the recovery rate and relative standard deviation (RSD). All measurements were repeated for 3 times.

Detection of FA in orange juice:

The orange juice samples were centrifuged at 8000 rpm for 20 min and filtered through a 0.22 μM microporous membrane. The working solution was prepared by diluting the sample solution with pure water to maintain the concentration of the working solution within the linear range. Then, different amount of FA were added into the above working solution to calculate the recovery rate and relative standard deviation (RSD). All measurements were repeated for 3 times.

9. Fluorescence detection of Cr(VI)

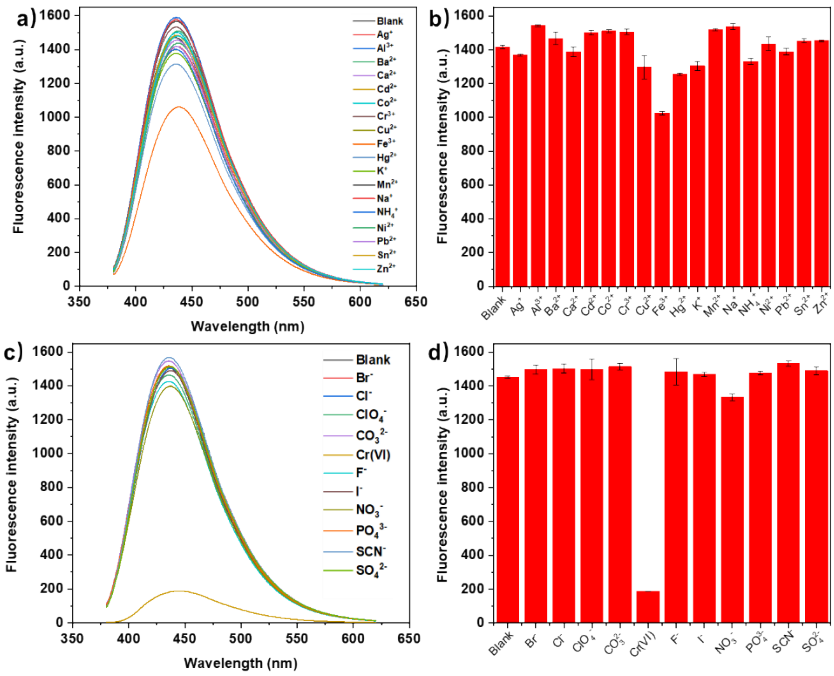

Fig. S5 Fluorescence spectra (a,c)/intensities (b,d) of N-GQDs (λex = 370 nm, λem = 445 nm) with different cations or anions (175 μM) (n = 3).

10. Response time of N-GQDs to Cr(VI)

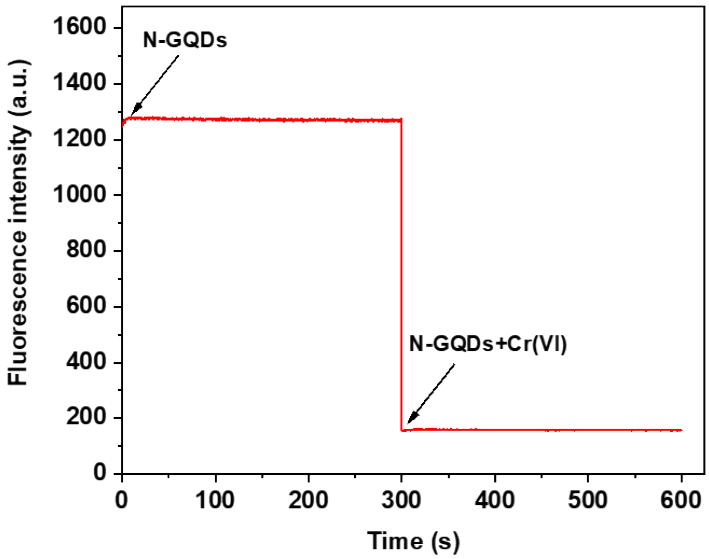

Fig. S6 Fluorescence intensity of N-GQDs (λex = 370 nm, λem = 445 nm) in the absence/presence of Cr(VI) (175 μM).

11. Photographs of N-GQDs solution with Cr(VI)

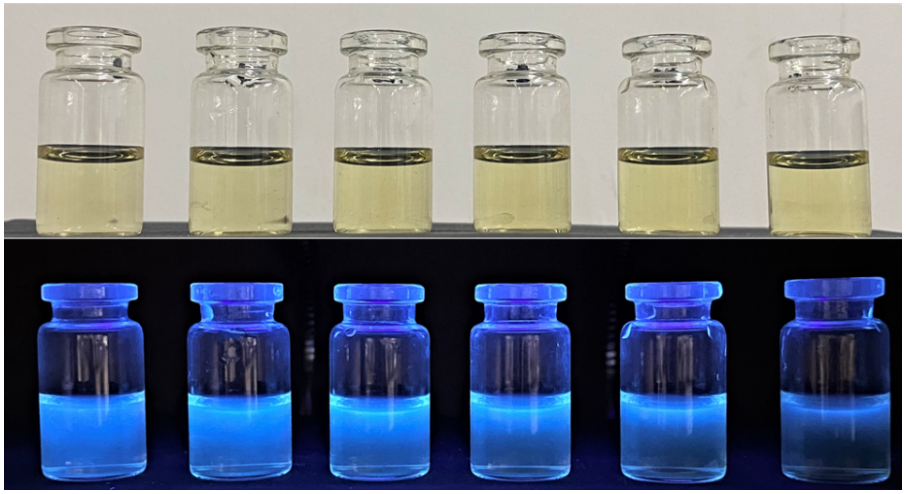

Fig. S7 Photographs of N-GQDs solution with Cr(VI) (from left to right: 0, 20, 40, 60, 80 and 100 μM) under fluorescent lamp (above) and 365 nm UV light (below).

12. Table S4 Fluorescence intensity and standard deviation

No.	Fluorescence Intensity (a.u.)	F/F_0
1	1310	1.0022
2	1312	1.0037
3	1308	1.0007
4	1309	1.0014
5	1304	0.9976
6	1307	0.9999
7	1302	0.9961
8	1302	0.9961
9	1311	1.0030
10	1306	0.9992
σ	**0.0026**	

13. Fluorescence detection of FA

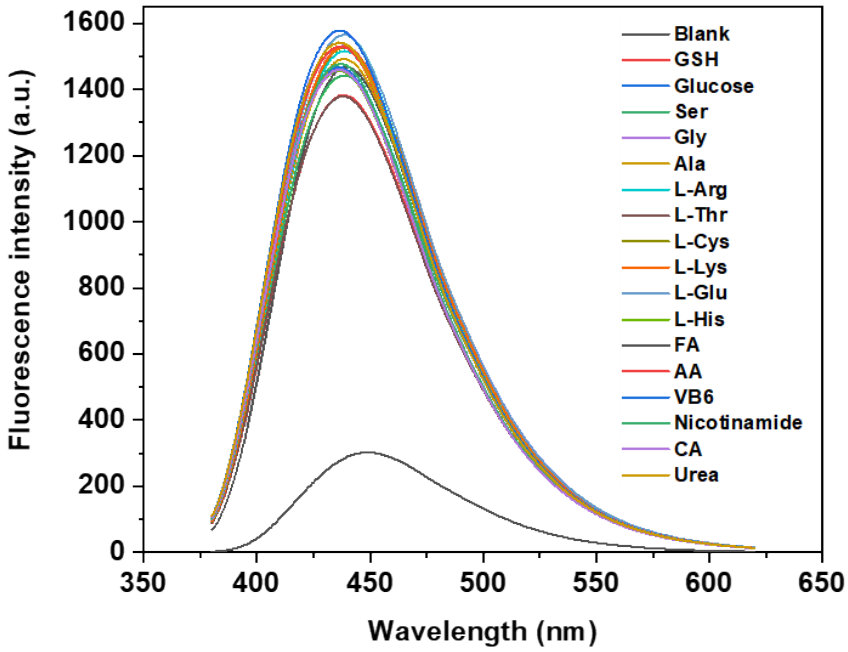

Fig. S8 Fluorescence spectra of N-GQDs (λex = 370 nm, λem = 445 nm) with different compounds (200 μM).

14. The response time of N-GQDs to FA

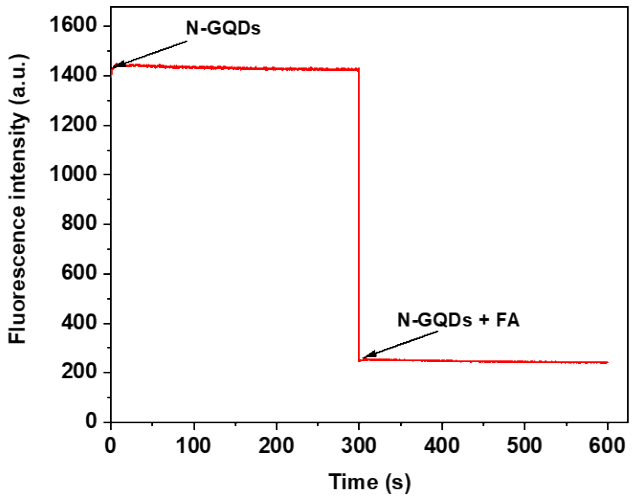

Fig. S9 Fluorescence intensity of N-GQDs (λex = 370 nm, λem = 445 nm) in the absence/presence of FA (200 μM).

15. Photographs of N-GQDs solution with FA

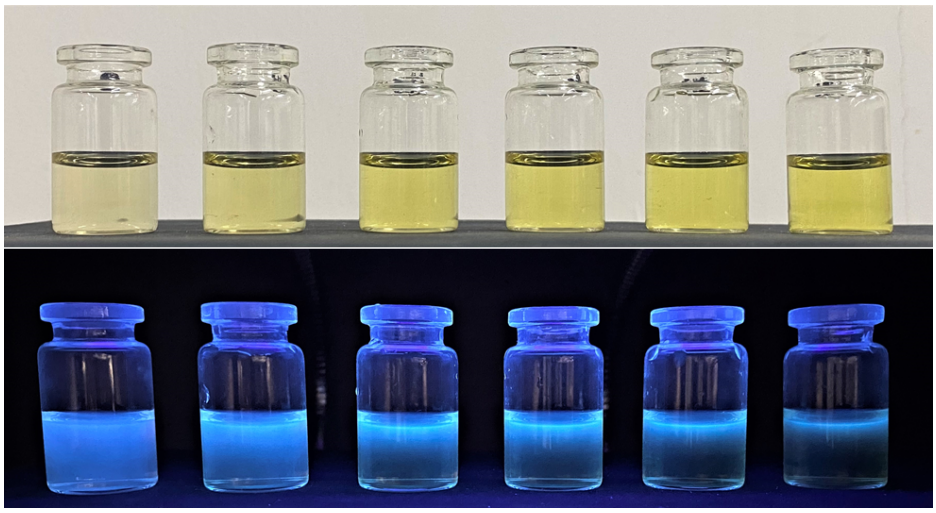

Fig. S10 Photographs of N-GQDs solution with FA (from left to right: 0, 20, 40, 60, 80 and 100 μM) under fluorescent lamp (above) and 365 nm UV light (below).

16. Exploration of the quenching mechanism by calculation methods.

A_{ex}, A_{em} and F_{obsd} are the absorbance and fluorescence intensities of N-GQDs at optimal excitation (Ex = 370 nm) and optimal emission (Em = 445 nm). F_{cor} (corrected fluorescence emission intensities of N-GQDs at 445 nm) was calculated according to Eq. 1 (the Parker's equation). Then, *CF* (correction factor), E_{obsd} (observed fluorescence suppression efficiency), E_{cor} (corrected fluorescence suppression efficiency) and $F_{cor.o}/F_{cor}$ (the ratio of corrected fluorescence emission intensities of N-GQDs at 445 nm without/with analytes) were calculated as shown in Table S5 and S6 (CF ≤ 3 to ensure the accuracy of the results). The IFE ratio was then calculated by (E_{obsd} - E_{cor})/ E_{obsd} to be 79.74% for Cr(VI) and 90.11% for FA.

The ratio of corrected fluorescence emission intensities of N-GQDs at 445 nm without/with analytes

($F_{cor.o}/F_{cor}$) versus the concentration of analytes were plotted as shown in Fig S10. In the presence of Cr(VI), $F_{cor,0}/F_{cor}$ has a linear relationship with the concentration of Cr(VI) (Fig. S10b), which indicates the presence of static quenching effect and dynamic quenching effect in the system according to Stern-Volmer equation (Eq. 2). While, $F_{cor,0}/F_{cor}$ was not linearly related to FA, which indicated that the static quenching effect and dynamic quenching effect between N-GQDs and FA are negligible.

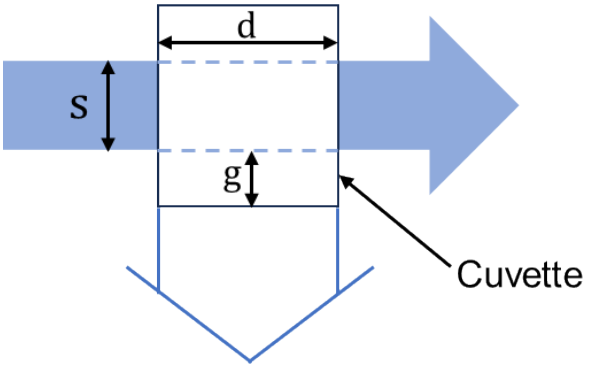

Fig. S11 Geometry of a quartz cuvette, where d, g and s are 1.00, 0.25 and 0.50 cm.

Table S5 Parameters used to calculate the IFE percentage of Cr(VI) to N-GQDs fluorescence

Cr(VI) (μM)	A_{ex}	A_{em}	CF	F_{obsd}	F_{cor}	E_{obsd}	E_{cor}	$F_{cor,0}/F_{cor}$
0	0.34	0.06	1.55	1004.17	1556.46	0.00	0.00	1.00
5	0.41	0.07	1.69	902.00	1524.38	0.10	0.02	1.02
10	0.49	0.09	1.85	806.13	1491.35	0.20	0.04	1.04
15	0.54	0.09	1.94	754.17	1463.08	0.25	0.06	1.06
20	0.59	0.10	2.03	699.57	1420.12	0.30	0.09	1.10
25	0.66	0.11	2.21	622.40	1375.50	0.38	0.12	1.13

$CF = F_{cor}/F_{obsd}$; E_{obsd} =1- F_{obsd} / $F_{obsd,0}$; E_{cor} =1- F_{cor} /$F_{cor,0}$

Table S6 Parameters used to calculate the IFE percentage of FA to N-GQDs fluorescence

FA (μM)	A_{ex}	A_{em}	CF	F_{obsd}	F_{cor}	E_{obsd}	E_{cor}	$F_{cor,0}/F_{cor}$
0	0.39	0.10	1.71	1008.30	1724.19	0.00	0.00	1.00
10	0.47	0.11	1.85	895.77	1657.19	0.11	0.04	1.04
15	0.52	0.11	1.95	854.80	1666.86	0.15	0.03	1.03
20	0.59	0.13	2.12	796.40	1688.37	0.21	0.02	1.02
25	0.64	0.13	2.22	740.33	1643.54	0.27	0.05	1.05

$CF = F_{cor}/F_{obsd}$; E_{obsd} =1- F_{obsd} / $F_{obsd,0}$; E_{cor} =1- F_{cor} /$F_{cor,0}$

$$\frac{F_{cor}}{F_{obsd}} = \frac{2.3dA_{ex}}{1-10^{-dA_{ex}}} 10^{gA_{em}} \frac{2.3sA_{em}}{1-10^{-sA_{em}}} \quad \text{(Eq. 1)}$$

F_{cor} *and* F_{obsd} are N-GQDs corrected and measured fluorescence intensities (Em = 445 nm); d, g and s are the geometric parameters of the quartz cuvette (Fig. S9) 1.00, 0.25 and 0.50 cm respectively; A_{ex} and A_{em} are the absorbance of N-GQDs at optimal excitation (Ex = 370 nm) and optimal emission (Em = 445 nm).

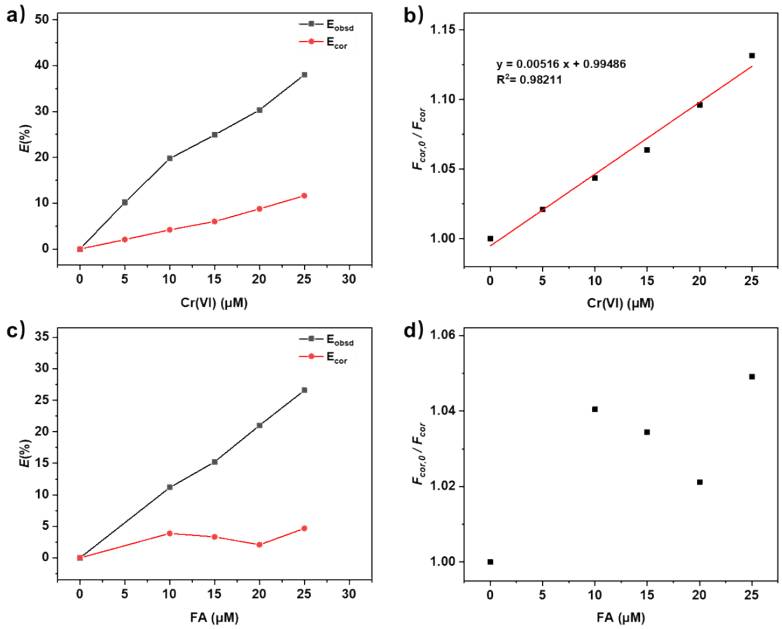

Fig. S12 Observed and corrected fluorescence intensity suppression efficiency (E_{obsd} and E_{cor}) (a,c); Relationship between Cr(VI) (b) or FA (d) concentrations and $F_{cor,0}/F_{cor}$.

$$F_{cor,0}/F_{cor} = 1 + K_{SV}[Q] \quad \text{(Eq. 2)}$$

$F_{cor,0}$ and F_{cor} are corrected fluorescence intensities without and with the addition of Cr(VI) or FA; K_{sv} is the Stern-Volmer constant; $[Q]$ is the concentration of Cr(VI) or FA.